

## RESEARCH ARTICLE

# IVIg attenuates complement and improves spinal cord injury outcomes in mice

Faith H. Brennan<sup>1</sup>, Nyoman D. Kurniawan<sup>2</sup>, Jana Vukovic<sup>1,3</sup>, Perry F. Bartlett<sup>3</sup>, Fabian Käsermann<sup>4</sup>, Thiruma V. Arumugam<sup>5</sup>, Milan Basta<sup>6</sup> & Marc J. Ruitenberg<sup>1,3,7</sup>

<sup>1</sup>School of Biomedical Sciences, The University of Queensland, Brisbane 4072, Australia

<sup>2</sup>Centre for Advanced Imaging, The University of Queensland, Brisbane 4072, Australia

<sup>3</sup>Queensland Brain Institute, The University of Queensland, Brisbane 4072, Australia

<sup>4</sup>Research, CSL Behring, Bern CH-3000, Switzerland

<sup>5</sup>Department of Physiology, Yong Loo Lin School of Medicine, National University of Singapore, 117597, Singapore

<sup>6</sup>BioVisions Inc., 9012 Wandering Trail Dr, Potomac, Maryland 20854, USA

<sup>7</sup>Trauma, Critical Care and Recovery, Brisbane Diamantina Health Partners, The University of Queensland, Brisbane 4072, Australia

## Correspondence

Marc J. Ruitenberg, School of Biomedical Sciences, The University of Queensland, Brisbane, QLD, 4072, Australia. Tel: +61 7 3346 7602; Fax: + 61 7 3365 1766; E-mail: m.ruitenberg@uq.edu.au

Milan Basta, BioVisions Inc., 9012 Wandering Trail Dr, Potomac, Maryland 20854, USA. Tel: +1 301 217 0740; Fax: +1 301 217 0740; E-mail: basta.milan@gmail.com

## Funding Information

This work was made possible by the Wings for Life Spinal Cord Research Foundation. M.J.R. was additionally supported by a SpinalCure Australia Career Development Fellowship, and the National Health and Medical Research Council of Australia (Project Grant 1060538). F.H.B. was supported by an Australian Postgraduate Award (The University of Queensland).

Received: 18 December 2015; Revised: 20 April 2016; Accepted: 21 April 2016

*Annals of Clinical and Translational Neurology* 2016; 3(7): 495–511

doi: 10.1002/acn3.318

## Abstract

**Objective:** Traumatic spinal cord injury (SCI) elicits immediate neural cell death, axonal damage, and disruption of the blood–spinal cord barrier, allowing circulating immune cells and blood proteins into the spinal parenchyma. The inflammatory response to SCI involves robust complement system activation, which contributes to secondary injury and impairs neurological recovery. This study aimed to determine whether intravenous immunoglobulin (IVIg), an FDA-approved treatment for inflammatory conditions, can scavenge complement activation products and improve recovery from contusive SCI. **Methods:** We used functional testing, noninvasive imaging, and detailed postmortem analysis to assess whether IVIg therapy is effective in a mouse model of severe contusive SCI. **Results:** IVIg therapy at doses of 0.5–2 g/kg improved the functional and histopathological outcomes from SCI, conferring protection against lesion enlargement, demyelination, central canal dilation, and axonal degeneration. The benefits of IVIg were detectable through noninvasive diffusion tensor imaging (DTI), with IVIg treatment counteracting the progressive SCI-induced increase in radial diffusivity (RD) in white matter. Diffusion indices significantly correlated with the functional performance of individual mice and accurately predicted the degree of myelin preservation. Further experiments revealed that IVIg therapy reduced the presence of complement activation products and phagocytically active macrophages at the lesion site, providing insight as to its mechanisms of action. **Interpretation:** Our findings highlight the potential of using IVIg as an immunomodulatory treatment for SCI, and the value of DTI to assess tissue damage and screen for the efficacy of candidate intervention strategies in preclinical models of SCI, both quantitatively and noninvasively.

## Introduction

Deregulated and chronically persisting inflammation in traumatic spinal cord injury (SCI) is thought to significantly exacerbate damage caused by the primary (mechanical) insult, and to also hamper endogenous repair processes.<sup>1</sup> Consequently, much research on so-called

secondary damage in SCI has focused on inflammation to better understand its role, and to define discrete therapeutic targets. Early studies showed that anti-inflammatory intervention with corticosteroids can confer neuroprotection and reduce edema in experimental SCI<sup>2</sup>; however, the clinical efficacy of this approach has been questioned.<sup>3</sup> Alternative immunomodulatory therapies

that are fast acting and more specific in targeting particular aspects of the complex neuroinflammatory response to SCI are therefore urgently needed.

One readily available candidate immunomodulatory therapy for SCI is intravenous immunoglobulin (IVIg), a blood product that contains mostly purified IgG from the pooled plasma of healthy human donors.<sup>4</sup> Although originally designed for antibody replacement therapy, IVIg is increasingly used to treat a variety of inflammatory/autoimmune conditions because of its potent anti-inflammatory effects and excellent safety record.<sup>5</sup> Proposed mechanisms of action for IVIg therapy in these conditions include scavenging and neutralization of complement activation products,<sup>6–11</sup> and regulation of F<sub>c</sub> receptor (F<sub>c</sub>R) signaling/expression,<sup>12</sup> both of which have been implicated in secondary immune-mediated SCI pathology.<sup>13–15</sup> Whether IVIg therapy can scavenge and neutralize complement activation products in SCI has, however, remained an outstanding question. Similarly, although there is already indication in the literature that IVIg therapy could be effective,<sup>16</sup> its immunomodulatory properties and the neuroprotection that this may afford have not been investigated in contusive SCI.

Aside from the need for new and effective immunomodulatory treatments in SCI, there is an additional unmet demand for transferable approaches that can assess treatment efficacy in both preclinical studies and human SCI patients. Proving the efficacy of promising new therapeutic interventions in clinical trials remains one of the biggest challenges in translational SCI research due to the heterogeneity in the patient population (i.e., differences in the initiating cause, lesion level, and severity).<sup>17</sup> Furthermore, although rodent SCI models replicate much of the etiology of human SCI, including the inflammatory response,<sup>18</sup> there are important intrinsic anatomical differences between species. Hence, the degree of recovery of locomotor function in quadruped animals may not automatically translate to bipedal humans.<sup>19</sup> We previously reported that in vivo diffusion tensor imaging (DTI) can quantitatively document the progression of secondary SCI pathology over time.<sup>20</sup> However, it remained unknown whether this noninvasive imaging technique is sensitive enough to also detect microstructural improvements in diffusion characteristics of the injured spinal cord following a therapeutic intervention.

In view of these outstanding questions, the primary aim of this study was to establish IVIg's dose–response relationship with regard to the neurological recovery and histopathological outcomes from contusive SCI. We further explored whether DTI was able to detect attenuated secondary SCI pathology with IVIg therapy. Finally, we investigated whether IVIg therapy has an attenuating

effect on the presence of inflammatory cells and complement activation products in the injured spinal cord.

## Materials and Methods

### Animals and procedures

**Mice.** A total of 99 wild-type (WT) C57BL6/J and 9 Emx1-creERT2:Rosa26-tdTomato mice on a C57BL6/J background were used in this study. All mice were females obtained from local breeding colonies (The University of Queensland Biological Resources), aged 8–10 weeks old and weighing between 18 and 21 grams at the time of surgery. Mice were maintained under standard conditions in clean holding facilities on a 12 h light–dark cycle with *ad libitum* access to food and water. All experimental procedures were approved by The University of Queensland's Animal Ethics Committee and conducted in accordance with the National Health and Medical Research Council of Australia's code of practice for the care and use of animals for scientific purposes, and the ARRIVE guidelines. All personnel involved in handling of the mice, behavioral testing, data collection, and analysis were blinded to the treatment of experimental groups for the duration of the study to avoid experimenter bias. A detailed description of all experimental methods and procedures is provided in Data S1.

### SCI and IVIg treatment

Mice were subjected to laminectomy (sham surgery) or contusive SCI as described previously.<sup>14</sup> Next, IVIg (CSL Behring – Privigen/Hizentra), or vehicle solution (250 mmol/L L-proline) was administered at 1 h after SCI while the mice were still under general anesthesia. For the dose–response studies, WT mice with SCI were randomly allocated to one of the following treatment groups: vehicle ( $n = 8$ ), 0.05 g/kg IVIg ( $n = 6$ ), 0.1 g/kg IVIg ( $n = 6$ ), 0.5 g/kg IVIg ( $n = 7$ ), 1 g/kg IVIg ( $n = 7$ ), or 2 g/kg IVIg ( $n = 7$ ). In a separate experiment, we also directly compared IVIg and albumin treatment to control for protein loading and/or associated changes in oncotic pressure as a contributing factor to therapeutic effectiveness. WT mice with SCI were again randomly allocated to intravenously receive human albumin (Sigma-Aldrich; 1 g/kg;  $n = 8$ ), 1 g/kg IVIg ( $n = 8$ ), or vehicle ( $n = 7$ ) as described above. For all studies, randomization was achieved through preprepared lists, with treatment allocation remaining concealed from investigators conducting the surgery. There were no significant differences in injury severity parameters (i.e., force and displacement) between experimental groups in any of the experiments at the outset ( $P > 0.05$ ; Table S1).

## Assessment of functional recovery, histopathology, and live imaging

Assessment of locomotor recovery was performed using the Basso Mouse Scale (BMS) at regular intervals post-SCI as previously described<sup>14</sup> and detailed in Data S1.

To determine whether intravenously administered Ig entered the spinal cord, immunofluorescent staining for human IgG (goat anti-hu-IgG, 1:100; Pierce Antibodies) was performed on sagittal tissue sections from sham-operated (i.e., laminectomy only;  $n = 3$ ) or SCI ( $n = 3$ ) mice that were killed 24 h after surgery. Primary antibody omission was used as a negative control for staining specificity. Hu-IgG staining was combined with immunofluorescent labeling of “Neuronal Nuclei” (NeuN) for neurons (mouse anti-NeuN, 1:200; Millipore), glial fibrillary acidic protein (GFAP) for astrocytes (rabbit anti-GFAP, 1:1000; Dako), ionized calcium binding adaptor protein 1 (Iba1) for microglia (rabbit anti-Iba1; 1:500, Wako), or the oligodendrocyte marker CC-1 (mouse anti-CC-1; 1:100, Abcam). Images were captured using a confocal microscope (Zeiss) with a Yokogawa spinning disk (CSU-W1), and then deconvolved using Huygens software (Scientific Volume Imaging). Postmortem assessment of histopathology (lesion volume and length, gliosis, and myelin preservation) was performed as detailed previously,<sup>14</sup> and described in Data S1. NF-200 staining was used to assess axonal sparing, and Emx1-creERT2:Rosa26-tdTomato mice with SCI ( $n = 9$ ; > 6 weeks post-tamoxifen induction) were employed to assess dieback of TdTomato<sup>+</sup> corticospinal tract (CST) axons as described in Data S1. Staining with Iba1, CD68 (rat anti-CD68; 1:200; Serotec), rat-anti-CD11b antibody (1:200, Serotec), and Hoechst nuclear dye was performed to assess the effect of IVIg therapy on macrophage density and activation as described in Data S1.

For in vivo DTI, SCI mice with a medium (1 g/kg) dose of IVIg therapy were subjected to longitudinal in vivo DTI prior to injury, and then again at 1, 7, and 35 days post-injury ( $n = 7$ ) as detailed previously.<sup>20</sup> Vehicle-treated spinal-injured mice were used as controls ( $n = 5$ ). DTI data were collected as detailed in Data S1. Regions of interest (ROIs) included the ventral funiculi (VF), lateral funiculi (LF), ventrolateral white matter (VLWM), and dorsal columns (DCs), all outlined on axial images as described previously.<sup>20</sup> *Ex vivo* DTI was performed at 35 days post-SCI for tractography purposes.<sup>20</sup>

## Western blot and ELISA

WT mice were subjected to SCI and randomly administered 1 g/kg IVIg or vehicle, at 1 h post-injury ( $n = 6$  per group). An additional five mice were subjected to sham surgery. At 1 day post-surgery, mice were killed with an overdose of

sodium pentobarbitone (100 mg/kg i.p., Virbac), after which the T11–T13 spinal cord segment was immediately dissected, snap frozen in liquid nitrogen, and stored at  $-80^{\circ}\text{C}$ ; blood plasma samples were also obtained. The Bio-Rad electroblotting system was used to examine the presence of C3b in homogenized spinal cord via western blot; C5a levels in these were quantified by ELISA (<sup>14</sup> and Data S1 for details).

## Statistical analysis

Data sets were analyzed using GraphPad Prism 6.0 software (GraphPad Software, Inc., La Jolla, CA, USA). Two-way, repeated measure analysis of variance (ANOVA) with Bonferroni *post hoc* test was used for longitudinal BMS, in vivo DTI data, and for spatial analysis of myelin, GFAP, macrophage content, and central canal size along the spinal axis. Two-sided Student's *t*-test was used for direct comparisons. One-way ANOVA with Newman–Keuls *post hoc* test was used for comparing endpoint BMS scores, lesion volumes, epicenter myelin, epicenter GFAP, neurofilament staining, ELISA, and western blot data. Pearson's correlation was used to determine the relationship between DTI parameters and BMS scores, and for DTI parameters with myelin content at 35 days post-injury. Experimental data are presented as scatter plots or group means; error bars indicate “standard error of the mean” (SEM). Appropriateness of sample sizes for key experimental groups was confirmed via a priori and *post hoc* power analysis, with power ( $1-\beta$ ) set at 0.80 and  $\alpha = 0.05$ .

## Results

### IVIg is present at the site of SCI and localizes to neurons and glia

We first determined whether IVIg entered into the spinal cord following contusive SCI. Immunofluorescent staining showed that exogenously administered Ig was present in the injured parenchyma at 24 h after surgery. Some hu-IgG immunoreactivity was present in sham-operated mice, but only in association with the leptomeninges (Fig. 1A) and small capillary-like structures inside the spinal cord (not shown), indicating that IVIg does not cross the uncompromised blood–spinal cord barrier. In sharp contrast, clear intraparenchymal hu-IgG staining was present following SCI, particularly at and around the lesion epicenter (Fig. 1B). Dual-color immunofluorescent staining revealed that, aside from a more diffuse distribution pattern throughout the damaged area, hu-IgG staining co-localized to surviving NeuN<sup>+</sup> neurons (Fig. 1C), GFAP<sup>+</sup> astrocytes (Fig. 1D), CC1<sup>+</sup> oligodendrocytes (Fig. 1E) as well as Iba1<sup>+</sup> microglia/macrophages (Fig. 1F).



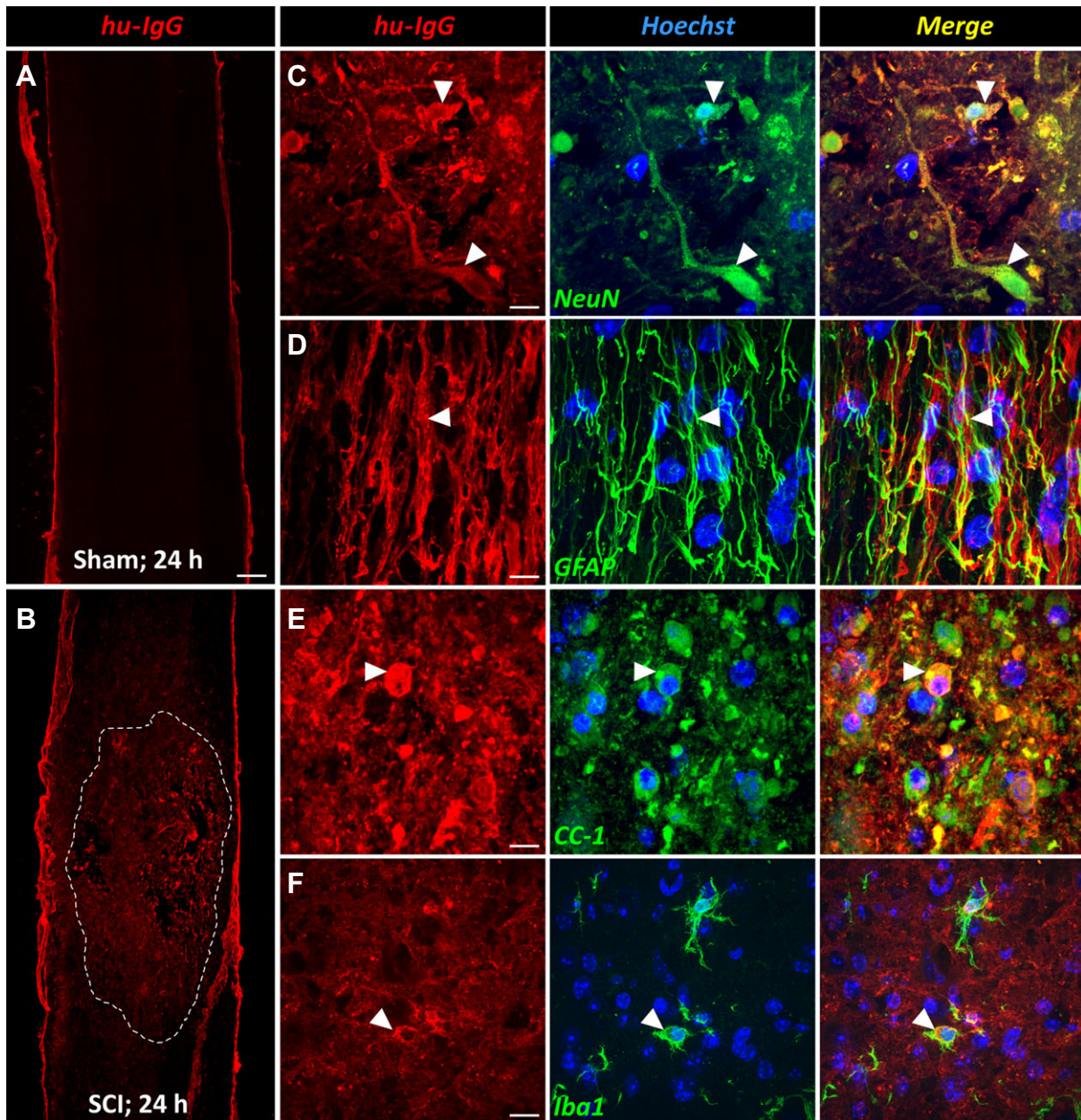


**Figure 1.** Intravenously administered immunoglobulins enter into the injured spinal cord. (A) Representative image of a sagittal spinal cord section from a sham-operated (i.e., laminectomy only) mouse that was injected with 1 g/kg intravenous immunoglobulin (IVIg) and perfused 24 h later. IVIg (hu-IgG staining; red) was detected near the meningeal border, but not within the spinal cord itself. (B) Mid-sagittal section of an IVIg-treated animal with SCI. Note that there is widespread immunoreactivity for hu-IgG across the injured segment, which then diminishes in intensity in both the rostral and caudal directions (the damaged area is outlined by the dotted white line). (C–F) Dual-color immunofluorescent staining showing co-localization between hu-IgG and NeuN<sup>+</sup> neurons (C, arrowheads), GFAP<sup>+</sup> astrocytes (D, arrowhead), CC1<sup>+</sup> oligodendrocytes (E, arrowhead), and Iba1<sup>+</sup> microglia (F, arrowhead). Scale bar: A, B (in A): 200  $\mu$ m; C: 15  $\mu$ m; D: 11  $\mu$ m; E: 13  $\mu$ m; F: 22  $\mu$ m. GFAP, glial fibrillary acidic protein; SCI, spinal cord injury.

**IVIg therapy improves SCI outcomes in a dose-dependent manner**

To explore the dose–response curve of IVIg in SCI, we performed BMS locomotor scoring with experimenter

blinding on cohorts of injured mice treated with IVIg doses ranging from 0.05 to 2 g/kg, or vehicle solution as a control. All mice displayed normal overground locomotion before surgery (BMS score of 9) and near-complete hind limb paralysis at 1 day post-SCI (Fig. 2A). By 7 days

post-injury, mice receiving the highest dose of IVIg (i.e., 2 g/kg) had recovered significantly more hind limb locomotor function than vehicle-treated controls ( $P = 0.018$ ; two-sided Student's *t*-test); a similar trend was observed for a 1 g/kg dose ( $P = 0.062$ ). By 14 days post-SCI, mice treated with IVIg doses of 0.5 g/kg or more had all diverged from the vehicle-treated control group. This trend continued and significant improvements in BMS scores were found with IVIg doses of 0.5 g/kg ( $P < 0.01$ ), 1 g/kg ( $P < 0.001$ ), or 2 g/kg ( $P < 0.01$ ) from 21 days post-SCI onward. Direct comparison of endpoint BMS scores (35 days post-SCI) confirmed that only higher doses of IVIg (0.5–2 g/kg) improved hind limb locomotor performance compared to vehicle controls (Fig. 2B; equal efficacy between doses). Lower doses of IVIg (i.e., 0.05 and 0.1 g/kg) did not show therapeutic efficacy ( $P \geq 0.12$ ).

Postmortem histopathological analyses at 35 days post-SCI confirmed improved outcomes with higher IVIg doses, with highly significant reductions in lesion volumes following treatment with either 0.5 g/kg (31% reduction;  $P < 0.0001$ ), 1 g/kg (34% reduction;  $P < 0.0001$ ), or 2 g/kg IVIg (27% reduction;  $P < 0.0001$ ). Although treatment with an IVIg dose of 0.1 g/kg did not lead to a significant improvement in BMS scores, we did observe a small (15%) reduction in lesion volume for this group ( $P < 0.05$ ; Fig. 2D). Similar trends were observed when analyzing lesion length, with IVIg doses of 0.5, 1 or 2 g/kg reducing the lesion progression along the spinal axis by 28%, 38%, and 30%, respectively (Fig. 2E).

Analysis of FluoroMyelin staining up to  $\pm 1.0$  mm away from lesion epicenter showed that, consistent with our observations regarding lesion volume, administration of IVIg at doses of 0.5 g/kg or above significantly improved myelin content/preservation within the VLWM between 600  $\mu\text{m}$  rostral and 700  $\mu\text{m}$  caudal of the lesion epicenter (Fig. 2F). At the lesion epicenter, higher dose (0.5–2 g/kg) IVIg therapy increased myelin preservation/presence by 50–60% compared to vehicle controls ( $P < 0.0001$ ; Fig. 2C and G). Consistent with the functional outcome, IVIg therapy at lower doses had little to no effect on myelin preservation. Specifically, only IVIg therapy at 0.1 g/kg showed modest efficacy, increasing myelin content at the lesion epicenter by 21% ( $P < 0.01$ ); this dose was, however, substantially less effective than higher doses of IVIg ( $P < 0.0001$ ).

Quantification of astroglial reactivity revealed clear signs of gliosis within  $\pm 800$   $\mu\text{m}$  of the lesion epicenter in vehicle-treated mice (Fig. 2C and H). Regardless of the dosing used, IVIg therapy did not affect astrogliosis at the lesion epicenter. Consistent with the observed reductions in lesion volume/length, a more confined astrogliotic response ( $\pm 500$ – $600$   $\mu\text{m}$ ) was observed following higher

dose (0.5 g/kg and above) IVIg treatment. “Area under the curve” analysis confirmed less widespread astrogliosis in these IVIg-treated groups compared to vehicle controls (Fig. 2I). IVIg treatment at  $\leq 0.1$  g/kg was not effective in reducing glial scarring.

Finally, we noticed that dilation of the central canal, a commonly observed phenomenon rostral to the site of SCI, appeared reduced in at least some animals. We therefore investigated whether treatment of SCI mice with an effective dose of IVIg ( $\geq 0.5$  g/kg) attenuated central canal dilation at 35 days post-injury (see Fig. S1). In vehicle-treated SCI controls, central canal areas were significantly increased between 300 and 600  $\mu\text{m}$  rostral to the lesion epicenter, up to a cross-sectional area of 0.051  $\text{mm}^2$  (25-fold increase over baseline); no such increases were seen caudal to the lesion site or further rostral, that is 700–1000  $\mu\text{m}$  away from the lesion epicenter, where the size of the central canal was typically less than 0.002  $\text{mm}^2$ . The central canal was not identifiable within  $\pm 100$   $\mu\text{m}$  of the epicenter regardless of the treatment condition. IVIg therapy at a dose of 1 g/kg significantly reduced central canal dilation rostral to the lesion site at 500  $\mu\text{m}$  ( $P < 0.05$ ), 400  $\mu\text{m}$  ( $P < 0.0001$ ) and 300  $\mu\text{m}$  ( $P < 0.01$ ; Fig. S1A and B). The maximally dilated area of the central canal (independent of its distance to the lesion epicenter) was also significantly lower in these mice compared to vehicle-treated controls ( $P < 0.05$ ; Fig. S1C). IVIg therapy at a dose of 0.5 g/kg or 2 g/kg also attenuated central canal dilation relative to vehicle-treated SCI controls, but only at 500  $\mu\text{m}$  ( $P < 0.05$ ) rostral to the lesion epicenter. Collectively, these data show that higher dose IVIg therapy consistently improves the functional and histological outcome from SCI, with a dose of 1 g/kg showing the least amount of intragroup variation. This dose was therefore used in all subsequent experiments.

### **IVIg therapy attenuates SCI-induced changes in fractional anisotropy and radial diffusivity**

Having established that IVIg therapy augments recovery, we next investigated whether these improvements were detectable with DTI (Fig. 3A). Longitudinal imaging revealed a progressive deterioration of fractional anisotropy (FA) values – a measure of tissue directionality and integrity<sup>20</sup> – in the VF and LF of vehicle-treated controls between 1 and 35 days post-SCI ( $P < 0.01$ ; Fig. 3B and C). Importantly, IVIg greatly attenuated the SCI-induced decline in FA values for both the VF ( $P < 0.01$ ) and LF ( $P < 0.05$ ). No time or treatment effect was observed for FA values in the DCs, that is the site of direct impact (Fig. 3D).



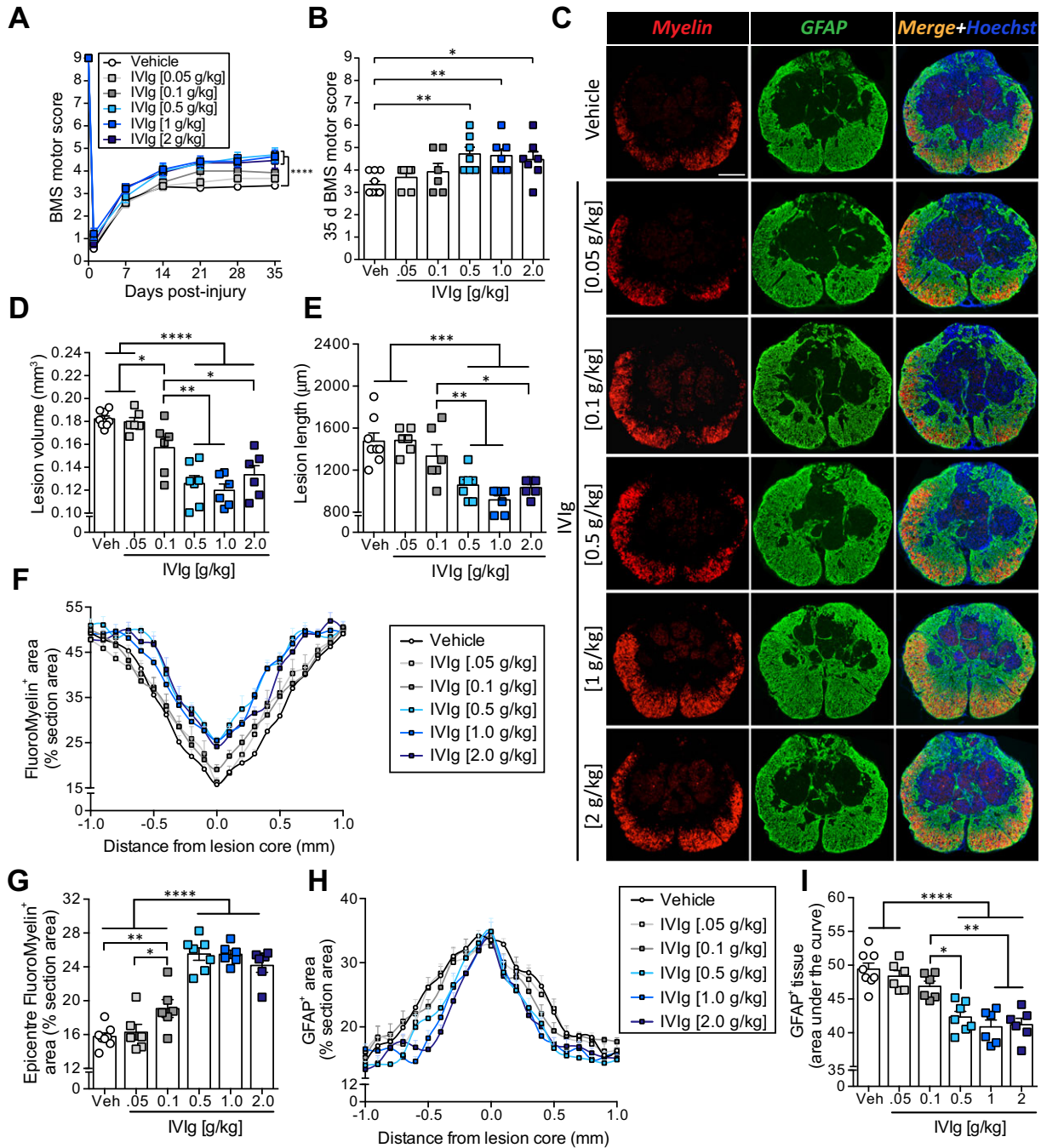


**Figure 2.** IVIg improves the outcome from experimental spinal cord injury (SCI). (A) Mice administered IVIg (0.5–2 g/kg) showed significantly improved hind limb motor recovery compared to vehicle-treated controls from 21 days post-SCI onwards. IVIg therapy at 0.1 g/kg or below did not improve SCI outcomes. (B) Scatter plot showing the spread of individual BMS scores for each of the experimental groups at 35 days post-SCI. (C) Representative sections of the lesion epicenter at 35 days post-injury for each of the experimental groups. (D, E) Mice administered IVIg (0.5–2 g/kg) showed significantly reduced lesion volume (D) and lesion length (E) compared to those administered either lower doses of IVIg or vehicle. (F, G) Analysis of myelin preservation showed that IVIg doses of  $\geq 0.5$  g/kg significantly increased the myelin content along the spinal axis (F) and at the lesion epicenter (G). (H, I) Quantification of GFAP immunostaining revealed a more confined gliotic response along the spinal axis with 0.5–2 g/kg IVIg therapy (H), as also confirmed by “area under the curve” analysis (I). (A, F, H) Mean ( $\pm$  SEM;  $n = 6-8$  per group;  $****P < 0.0001$ ; two-way repeated measure analysis of variance (ANOVA) with Bonferroni *post hoc* test. (B, D, E, G, I) Mean  $\pm$  SEM;  $*P < 0.05$ ;  $**P < 0.01$ ;  $***P < 0.001$ ;  $****P < 0.0001$ ; one-way ANOVA with Newman–Keuls *post hoc* test;  $n = 6-8$  per group. Scale bar, c (top left): 200  $\mu$ m. BMS, Basso Mouse Scale; GFAP, glial fibrillary acidic protein.

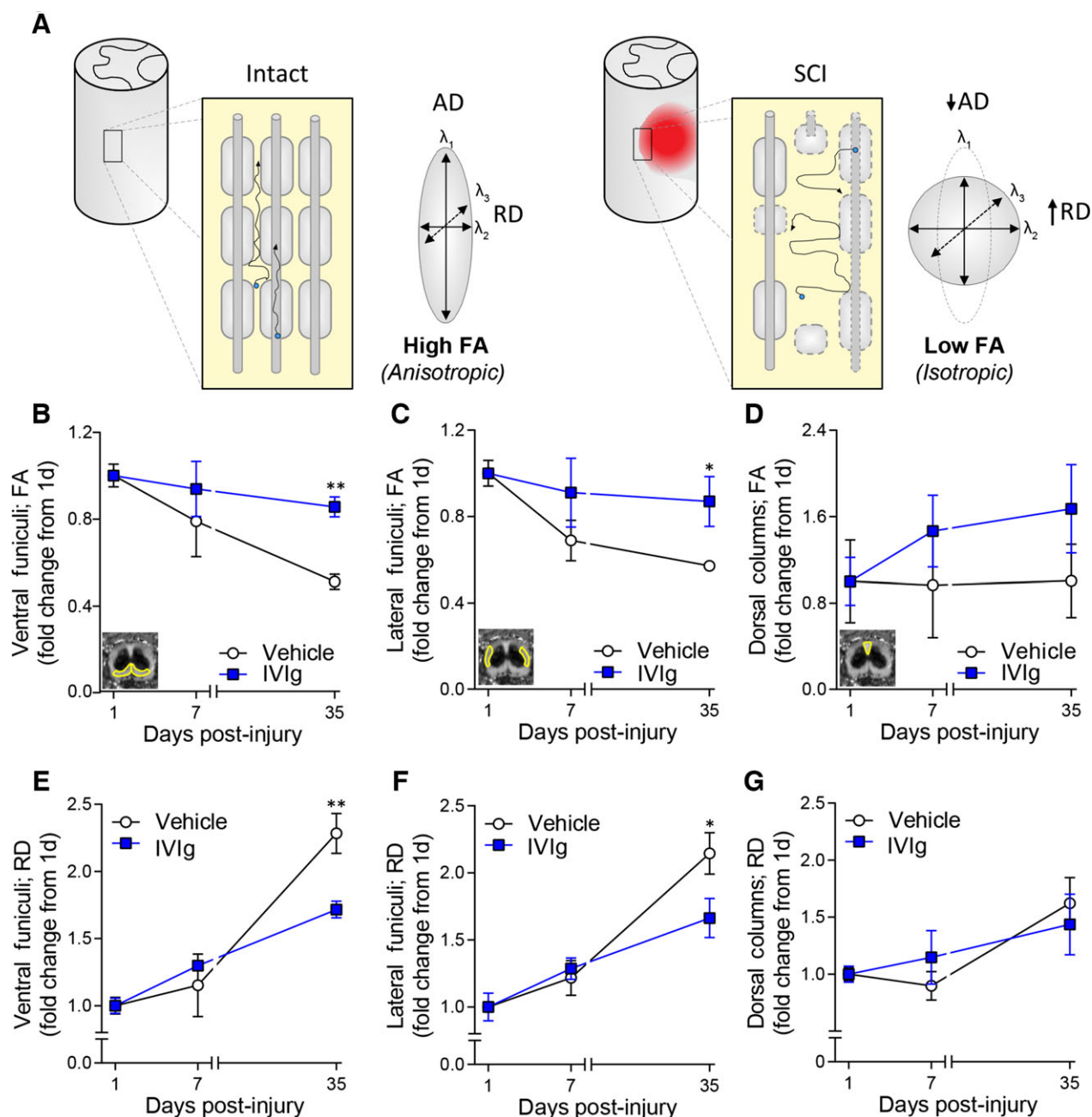


**Figure 3.** IVIg treatment improves diffusion tensor imaging (DTI) measures. (A) Schematic diagram explaining anisotropic and isotropic diffusion in spinal white matter based on DTI principles. Blue dots indicate water molecules and their net trajectory of diffusion (arrows) as influenced by the cytoarchitecture of the spinal cord white matter under homeostatic and injured conditions. Diffusion of molecules in the spinal white matter is normally highly restricted (anisotropic) by anatomical barriers such as axonal membranes and myelin sheaths (*left*). Axonal damage and loss of myelin following spinal cord injury (SCI) (*right*) disrupts these barriers, leading to less directional (isotropic) diffusion, lower fractional anisotropy (FA), and higher radial diffusivity (RD). (B–D) Temporal change in FA at the lesion epicenter for the ventral funiculi (VF; B), lateral funiculi (LF; C), and the dorsal columns (DCs; D). Note the deterioration of FA values in the VF and LF of vehicle-treated mice between 1 and 35 days post-SCI, and that IVIg treatment attenuated this pathological change in FA values for these ROIs. No significant temporal change in FA values was observed for the DCs in either experimental group. (E–G): Note the increase in RD between 1 and 35 days post-SCI at the lesion epicenter for both the VF (E) and LF (F). IVIg treatment significantly counteracted these SCI-induced increases in RD. As with FA, no significant time or treatment effect was observed for RD values in the DC area (G). All data points represent mean  $\pm$  SEM;  $n = 5$ –7 per experimental group; \* $P < 0.05$ ; \*\* $P < 0.01$ ; two-way repeated measures ANOVA with Bonferroni *post hoc* test. ANOVA, analysis of variance.

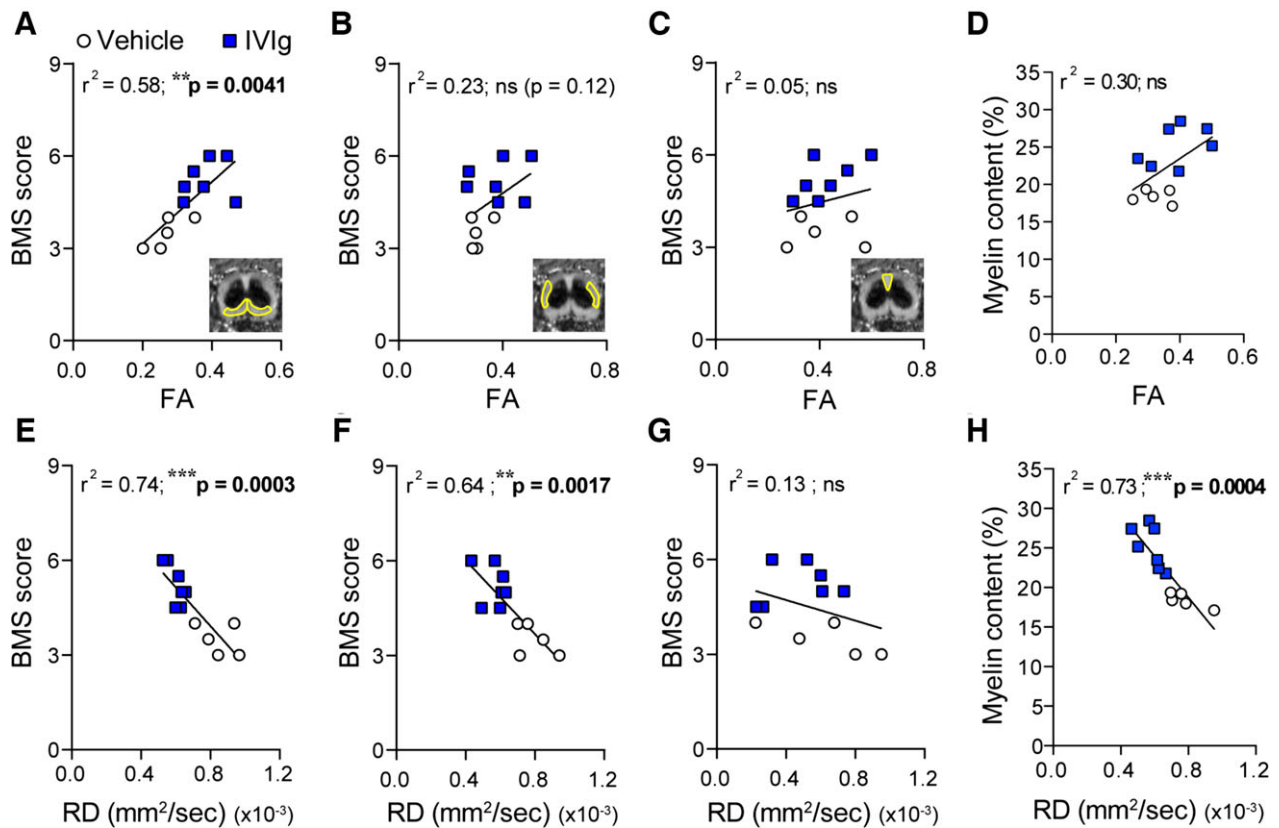


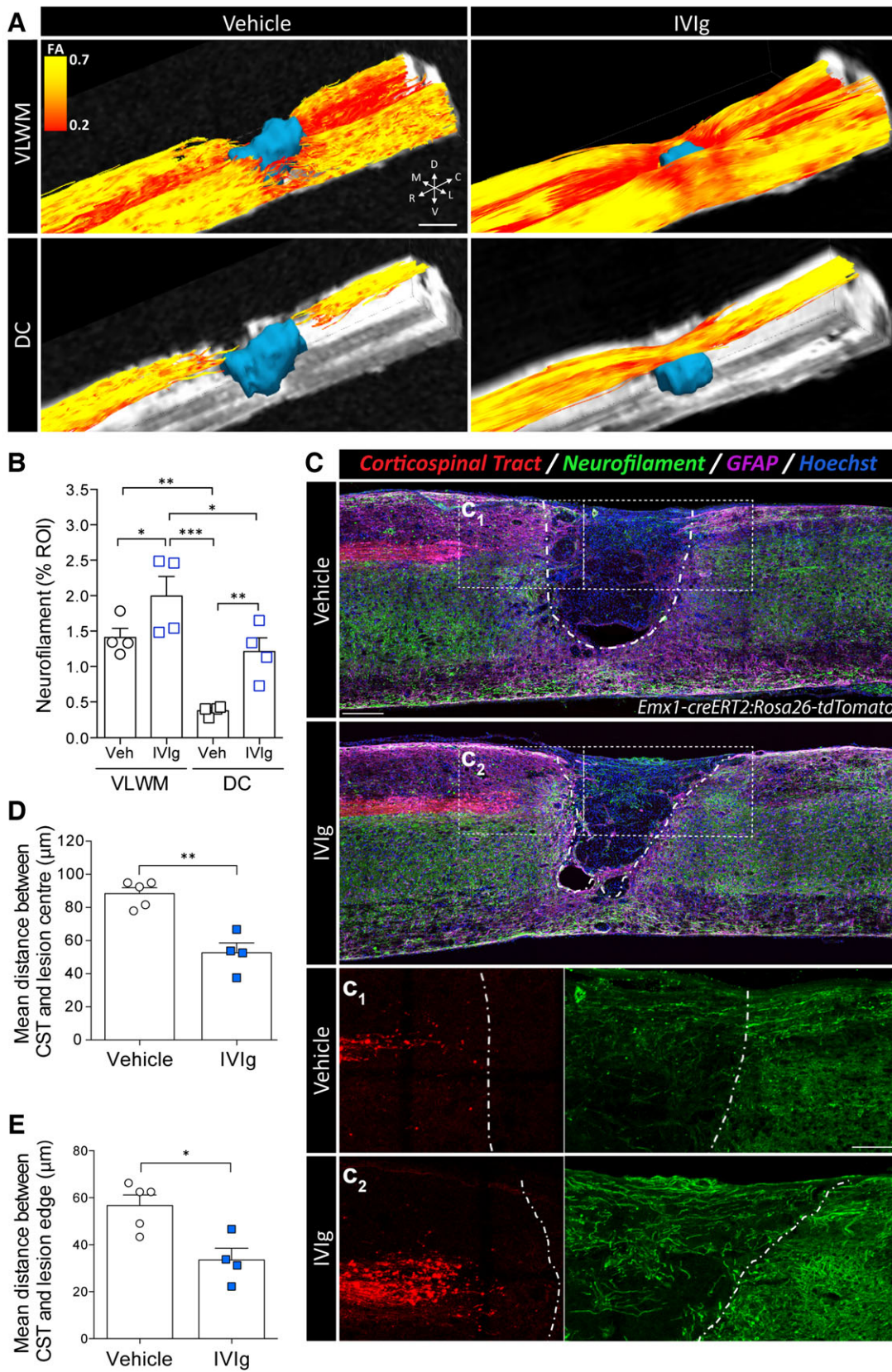
**Figure 4.** Endpoint DTI measures correlate with Basso Mouse Scale (BMS) scores and myelin content. Blue squares are data points for individual mice within the IVIg-treated group; vehicle-treated spinal cord injury (SCI) controls are shown as white circles. Trend lines based on regression analysis are shown in black for each graph. (A–C): fractional anisotropy (FA) values in the VF (A), but not LF (B) or the DCs (C), were significantly correlated with BMS scores at 35 days post-SCI for the cohort. (D) FA values for the combined ventrolateral white matter (VLWM) were trending but nonsignificantly (ns) correlated with myelin content ( $P = 0.063$ ). (E–G): Endpoint radial diffusivity (RD) values in the VF (E) and the LF (F), but not the DCs (G), tightly correlated with final BMS scores (35 days post-injury). (H) RD values for the VLWM were also strongly correlated with myelin content at 35 days post-SCI. Linear regression with Pearson correlation;  $n = 5$ – $7$  per experimental group;  $*P < 0.05$ ;  $**P < 0.01$ ;  $***P < 0.001$ . DTI, diffusion tensor imaging.

Progressive secondary SCI pathology includes immune-mediated mechanisms (i.e., autoantibodies, complement activation, and  $F_c$  receptors), which contribute to demyelination of affected white matter pathways.<sup>13</sup> As the myelin sheath normally restricts

perpendicular diffusion, changes in myelin structure are best reflected by changes in radial diffusivity (RD).<sup>21</sup> We therefore reasoned that SCI-induced changes in RD values for the VLWM should be attenuated if IVIg treatment was indeed protecting against secondary

**Figure 5.** IVIg treatment results in axonal sparing/regrowth and attenuates corticospinal tract (CST) dieback. (A) Representative tractography images, color-coded by FA, showing improved streamline continuity in the ventrolateral white matter (VLWM) and dorsal columns (DCs) following IVIg treatment (1 g/kg). (B) Quantitative analysis of neurofilament (NF-200) staining in transverse sections at the lesion epicenter. Note that IVIg treatment significantly increased NF200<sup>+</sup> profiles in the VLWM and the DCs compared to vehicle controls. (C) Representative mid-sagittal sections of *Emx1-creERT2;Rosa26-tdTomato* mice at 35 days post-SCI. Note the qualitative reduction in lesion size following IVIg treatment. The dashed white line indicates the lesion border as delineated by glial fibrillary acidic protein (GFAP) staining.  $C_1$ ,  $C_2$ : Higher power images of the boxed regions in C, showing attenuated CST dieback rostral to the lesion (red, left) and an increased presence of NF200<sup>+</sup> profiles (green, right) in the lesion core (GFAP<sup>-</sup> area) of IVIg-treated mice. (D, E) Quantification of CST dieback relative to both the lesion epicenter (D) and the lesion edge (E). All data are presented as mean  $\pm$  SEM. (B)  $n = 4$  per experimental group;  $*P < 0.05$ ;  $**P < 0.01$ ;  $***P < 0.001$ ; one-way ANOVA with Newman–Keuls *post hoc* test. (D, E)  $n = 4$ – $5$  per experimental group;  $*P < 0.05$ ;  $**P < 0.01$ ; Student's two-sided t-test. Scale bars: A (top left panel): 500  $\mu$ m; C (bottom, top-right panel): 250  $\mu$ m;  $C_1$ ,  $C_2$  (in  $C_1$ ): 130  $\mu$ m. Abbreviations (in A): C: caudal, D: dorsal, L: lateral, M: medial; R: rostral; V: ventral. ANOVA, analysis of variance; FA, fractional anisotropy; SCI, spinal cord injury.





immune-mediated demyelination. The increase in RD values following SCI was indeed significantly countered by IVIg treatment in both the VF ( $P < 0.01$ ; Fig. 3E) and LF ( $P < 0.05$ ; Fig. 3F) at 35 days post-injury. As with FA, no temporal change and/or treatment effect was observed for the DCs ( $P > 0.05$ ; Fig. 3G).

### FA and RD values in VLWM correlate with functional performance

Having established that DTI can reveal treatment efficacy, we next explored whether the various diffusion indices (i.e., FA, Axial diffusivity [AD], and RD) directly correlated with established primary (functional) and secondary (histopathological) outcome measures at the study endpoint (35 days post-SCI). BMS scores were positively and significantly correlated with FA values in the VF (Fig. 4A), but not the LF (Fig. 4B) or the DCs (Fig. 4C). AD values – an indicator of axonal integrity/damage – for these ROIs did not correlate with the functional performance of individual mice under the imaging conditions used (data not shown). RD values, on the other hand, were strongly and inversely correlated with BMS scores for both the VF (Fig. 4E) and LF (Fig. 4F), but not the DC area (Fig. 4G). RD (but not FA) measurements also significantly correlated with the myelin content of the VLWM at the lesion epicenter (Fig. 4D and H).

### IVIg therapy reduces axonal loss following contusive SCI

The beneficial effects of IVIg therapy in SCI were similarly evident from better tractography (Fig. 5A). Somewhat surprisingly, given that no time or treatment effect was observed for any of the diffusion indices in the presumptive DC region, a clear continuity of fiber tracks across the lesion was observed here in IVIg-treated animals. This observation prompted us to compare neurofilament staining in postmortem samples from each of the experimental groups to determine if IVIg therapy led to axonal sparing/regrowth. In agreement with the tractography data, SCI mice treated with 1 g/kg IVIg had significantly more neurofilament staining at the lesion epicenter, not only within the spared VLWM but also dorsally in the presumptive DC area (Fig. 5B). As the dorsal funiculus of the rodent spinal cord contains both ascending sensory axons (DC-medial lemniscus pathway) and descending motor fibers of the main CST, we used *Emx1-creERT2;Rosa26-tdTomato* mice to distinguish between these pathways in vivo in animals that were treated with either vehicle or 1 g/kg IVIg. A significant increase in the number of neurofilament<sup>+</sup> profiles was

again qualitatively observed following IVIg treatment, but no continuity of tdTomato-labeled CST fibers was seen across the lesion site (Fig. 5C). IVIg treatment did, however, lead to a significant reduction in the dieback of CST axons, irrespective of whether this was measured from the lesion epicenter ( $P < 0.01$ ; Fig. 5D) or the lesion edge ( $P < 0.05$ ; Fig. 5E), with the latter ruling out differences in lesion size between experimental groups as a potential confounding factor.

### IVIg attenuates presence of activated macrophages and complement activation products in SCI

Based on its known anti-inflammatory effects, we reasoned that IVIg therapy might have reduced demyelination, axonal dieback, and improved functional recovery, through a positive modulation of the inflammatory response. Quantification of activated microglia/macrophages (Iba1<sup>+</sup>CD68<sup>+</sup>Hoechst<sup>+</sup> cells) in the VLWM at 35 days post-SCI revealed that IVIg treatment (1 g/kg) significantly reduced the presence of Iba1<sup>+</sup>CD68<sup>+</sup>Hoechst<sup>+</sup> cells at and around the epicenter (100  $\mu$ m rostral to 500  $\mu$ m caudal) compared to controls (Fig. 6A and B).

As IVIg can scavenge/neutralize complement activation products,<sup>7–11</sup> and given the direct link between complement system activation and the magnitude of the inflammatory response in SCI,<sup>14</sup> we next explored whether IVIg therapy had an attenuating effect on the presence of complement activation products. Consistent with our previous findings, SCI (with vehicle treatment) significantly increased the levels of complement activation product C5a within the spinal cord at 1 day post-injury ( $P < 0.01$  compared to sham-operated controls; Fig. 6C); treatment with 1 g/kg IVIg counteracted this SCI-induced increase. Notably, similar results were obtained if C5a levels were measured as either absolute amounts, or relative to the weight of the dissected spinal cord segment for each sample ( $P < 0.05$ ; data not shown). Tissue levels of C3b, another complement activation product that rose by ~300% as a result of SCI ( $P < 0.001$ ), were also significantly reduced following IVIg treatment (Fig. 6D). Lastly, IVIg therapy does not appear to act via overconsumption of complement,<sup>11</sup> as circulating C5a levels in the plasma were not different between vehicle and IVIg-treated SCI mice (Veh:  $4.38 \pm 0.76$  vs. IVIg:  $3.70 \pm 0.42$  ng/mL; mean  $\pm$  SEM;  $n = 7–8$  per group).

### IVIg therapy is more effective than albumin in improving SCI outcomes

We finally sought to confirm that the benefits of IVIg therapy were indeed mediated by immunomodulatory



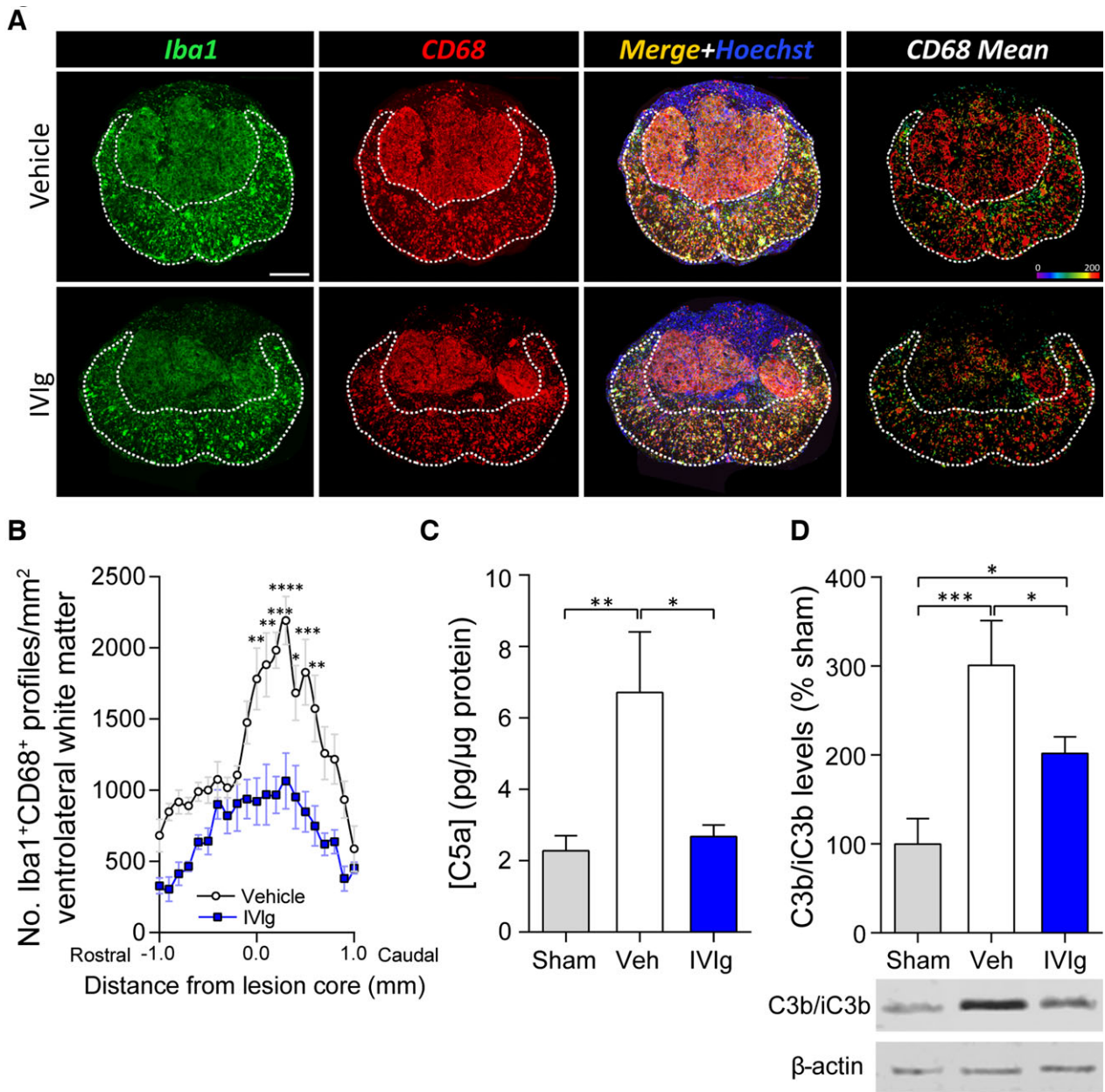


**Figure 6.** IVIg treatment reduces intraspinal presence of activated macrophages and complement activation products. (A) Representative histological sections of the lesion epicenter at 35 days post-spinal cord injury (SCI) from vehicle-treated controls (top row) or mice administered IVIg (1 g/kg) (bottom row). The dotted white line delineates the area of spared tissue. The “CD68 Mean” panels (right column) show the mean area (pixel units) of CD68 staining per Iba1+CD68+Hoechst+ cell. (B) Note that IVIg treatment significantly reduced the number of Iba1+CD68+Hoechst+ cells in the VLWM in sections within 100 μm rostral to 500 μm caudal of the lesion epicenter. (C) Analysis of C5a levels in the injured spinal cord segment at 1 day post-injury. Note the reduction in tissue C5a levels following IVIg treatment of SCI mice. (D) Western blot data from spinal cord homogenates of SCI mice showing that IVIg treatment also attenuated tissue C3b levels. (B) Mean ± SEM; \**P* < 0.05; \*\**P* < 0.01; \*\*\**P* < 0.001; \*\*\*\**P* < 0.0001; two-way analysis of variance (ANOVA) with Bonferroni *post hoc* test; *n* = 6–7. (C, D) Mean ± SEM; \**P* < 0.05; \*\**P* < 0.01; \*\*\**P* < 0.001; one-way ANOVA with Newman–Keuls *post hoc* test; *n* = 5–6. Scale bar: A (top left): 200 μm.

mechanisms and not just resulting from addition of a protein reserve.<sup>22</sup> For this, we directly compared the therapeutic efficacy of IVIg against albumin treatment. SCI mice were randomly assigned to either IVIg (1 g/kg),

albumin (1 g/kg), or vehicle treatment, all of which were delivered 1 h post-SCI. Similar to our observations in the dose–response study, mice treated with 1 g/kg IVIg recovered significantly more hind limb locomotor function



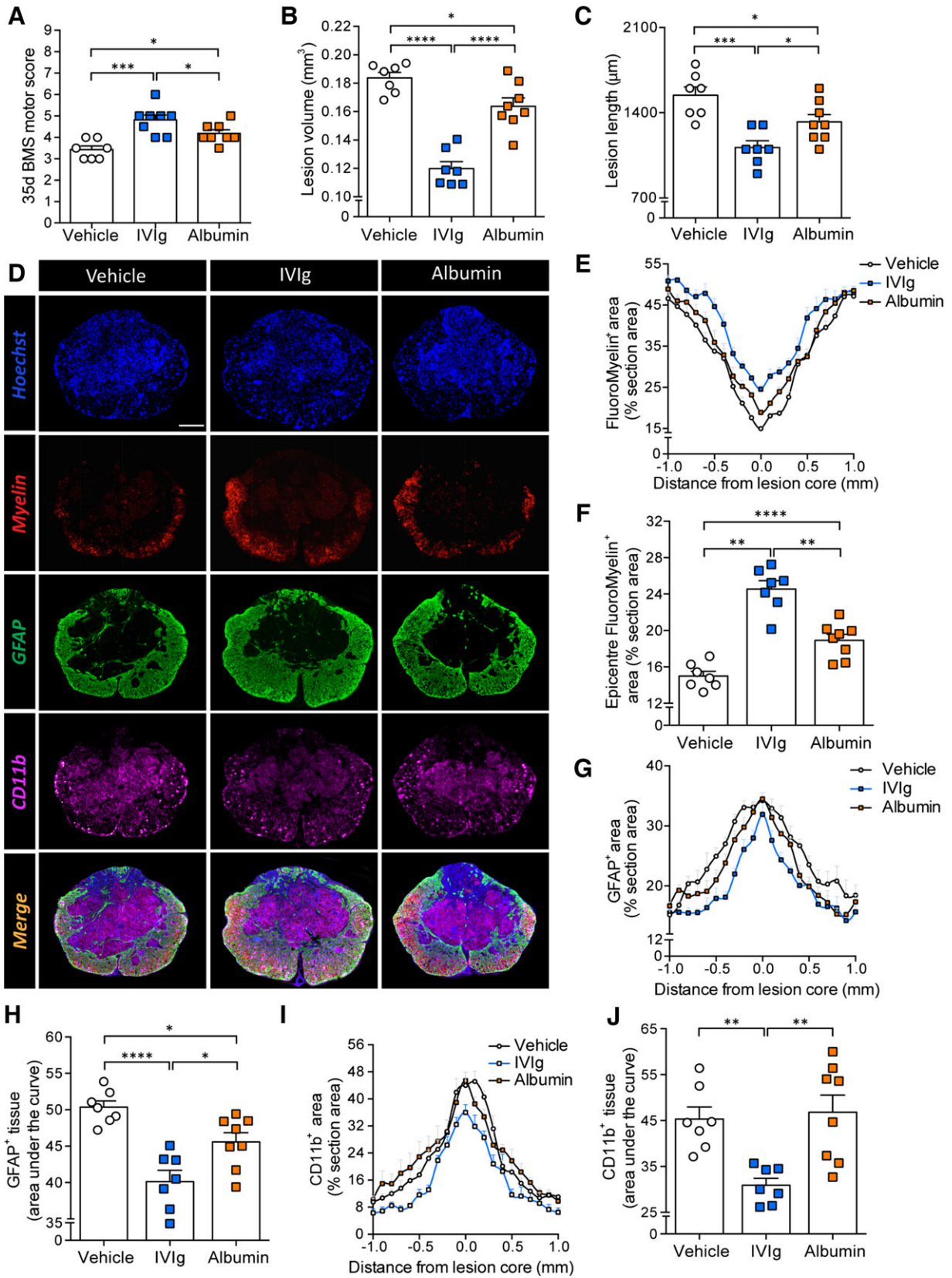


**Figure 7.** IVIg is more effective than albumin in improving spinal cord injury (SCI) outcomes. (A) Endpoint BMS locomotor scores showing that IVIg significantly improves the functional recovery compared to both vehicle- and albumin-treated SCI mice. (B, C) IVIg therapy also significantly reduced lesion volume (B) and lesion length (C) compared to both vehicle and albumin treatment. (D) Representative sections of the lesion epicenter at 35 days post-SCI for each of the experimental groups. (E, F) IVIg treatment resulted in increased myelin, around (E) and at (F) the lesion epicenter (35 days post-SCI). Note the significantly improved outcomes compared to both vehicle and albumin treatment (F). (G, H) Analysis of GFAP immunoreactivity around the lesion site (G) showed more confined astrogliosis in IVIg-treated mice compared to either vehicle or albumin treatment. “Area under the curve” analysis confirmed this result (H). (I, J) Spatial analysis of CD11b staining up to 1 mm on either side of the lesion epicenter (I) indicated that only IVIg treatment significantly reduced the CD11b<sup>+</sup> infiltrate at the lesion epicenter, which was again confirmed by “area under the curve” analysis (J). All data are presented as mean  $\pm$  SEM. (A–C, F, H, J) \* $P$  < 0.05; \*\* $P$  < 0.01; \*\*\* $P$  < 0.001; \*\*\*\* $P$  < 0.0001; one-way ANOVA with Newman–Keuls *post hoc* test;  $n$  = 7–8 per experimental group. Scale bar: D (top left): 200  $\mu$ m. ANOVA, analysis of variance. BMS, Basso Mouse Scale; GFAP, glial fibrillary acidic protein.

than vehicle-treated SCI controls ( $P$  < 0.001; Fig. 7A). Albumin treatment also led to a modest improvement in SCI outcomes, but this effect was inferior to IVIg therapy ( $P$  < 0.05; Fig. 7A).

Consistent with functional outcomes, lesion volumes of IVIg mice were again significantly smaller (35%,  $P$  < 0.0001; Fig. 7B) than those of vehicle-treated controls. Albumin treatment led to a much more modest change in lesion volume (11%;  $P$  < 0.05) and these were still 27% larger than those of IVIg-treated animals ( $P$  < 0.0001). A similar trend was observed for spread of the lesion along the length axis of the spinal cord (Fig. 7C), with IVIg therapy producing the most dramatic reduction in lesion length (28%;  $P$  < 0.001). This effect was again superior to that of albumin administration (14%;  $P$  < 0.05). As a result, the average length of the lesion was significantly greater (16%) in albumin-treated mice compared to those administered IVIg ( $P$  < 0.05).

Additional histological analysis once again confirmed an effect of IVIg therapy on myelin content/preservation up to 700  $\mu$ m rostral and 800  $\mu$ m caudal to the lesion epicenter (Fig. 7D and E); epicenter myelin was significantly increased by 64% ( $P$  < 0.0001) compared to vehicle, and 30% ( $P$  < 0.01) for albumin-treated SCI mice, respectively. Albumin itself also improved myelin content compared to vehicle-treated SCI controls but only within 200  $\mu$ m of the lesion epicenter (Fig. 7E), with a 26% improvement in myelin content at the lesion epicenter ( $P$  < 0.01; Fig. 7F). Similar to the dose–response studies, IVIg-treated animals again showed a more confined astroglial response, not only compared to vehicle treatment (21%,  $P$  < 0.0001) but also albumin (12%,  $P$  < 0.05; Fig. 7G and H). We lastly quantified CD11b staining to assess the presence of activated inflammatory macrophages (and neutrophils) at the lesion (Fig. 7D, I and J). Only IVIg therapy had a significant effect on the CD11b<sup>+</sup> infiltrate at the lesion site, showing a > 30% reduction compared to both vehicle and albumin-treated animals ( $P$  < 0.01; Fig. 7J). IVIg therapy was thus superior to albumin treatment in all primary

(functional) and secondary (histopathological) outcome measures.

## Discussion

IVIg is increasingly being utilized for the treatment of inflammatory/autoimmune disorders because of its potent immunomodulatory properties. IVIg therapy has already shown great promise in several models of acquired CNS injury,<sup>23–25</sup> but this study demonstrates its robust efficacy in counteracting secondary immune-mediated pathology in contusive SCI. We also show, for the first time, that IVIg therapy has a remarkable attenuating effect on the presence of complement activation products within the injured spinal cord, thereby providing clues as to how IVIg augments neurological recovery following neuro-trauma.

All of the clinically recommended doses for IVIg therapy (0.5–2 g/kg) improved SCI outcomes at endpoint, although only 2 g/kg enhanced recovery in the subacute phase (7 days post-injury). Aside from augmenting neurological recovery, IVIg therapy ( $\geq$  0.5 g/kg, delivered 1 h post-SCI) also reduced lesion volume and length, improved myelin content at and around the lesion epicenter, and led to more confined astrogliosis. Medium to high-dose IVIg additionally attenuated central canal enlargement rostral to the injury site, suggesting improved flow of cerebrospinal fluid around the lesion.<sup>26</sup> To the best of our knowledge, these data provide the first evidence that central canal expansion rostral to the site of contusive SCI is influenced by inflammatory processes. Low-dose IVIg treatment (0.05 or 0.1 g/kg) did not improve the primary (functional) outcome relative to vehicle treatment. The present findings independently support and extend from a previous study on the longer term benefits of human IgG treatment (0.4 g/kg, delivered 15 min post-injury) following clip compression injury.<sup>16</sup> Future studies should now explore the therapeutic window for IVIg therapy ( $\geq$ 0.5 g/kg) beyond the 1-h time point.

With an increasing number of promising therapeutic interventions under development and/or already being tested in human SCI,<sup>27</sup> there is an urgent need for noninvasive and transferable methods to assess treatment efficacy between animal and human studies and/or to also better account for patient heterogeneity in lesion severity at the outset.<sup>17</sup> Based on a growing body of evidence in support of DTI being one such technique,<sup>28–30</sup> we explored whether longitudinal *in vivo* DTI could detect the beneficial effects of IVIg therapy in live subjects. DTI can detect regions of edema, hemorrhage, axonal damage and/or demyelination, and Wallerian degeneration.<sup>31</sup> However, no study to date has evaluated whether DTI is sensitive enough to reveal microstructural improvements in tissue integrity as a result of treatment and, if so, how quantifiable changes in diffusion indices correlate with the current “gold standards” for assessing experimental treatment efficacy, that is, functional performance in open field (BMS scores) and histopathological analysis of post-mortem tissue samples.

Consistent with reports from previous human and experimental animal studies, including our own,<sup>20,32</sup> FA values were acutely reduced at the lesion epicenter (1 day post-SCI) but did not differ between groups. These early changes in FA are mostly driven by acute reductions in AD and reflect the primary impact of SCI, that is, large-scale axonal damage.<sup>1</sup> The decline in FA values during the more chronic phase of SCI is primarily driven by a progressively increasing RD and not AD-associated changes.<sup>20</sup> Remarkably, the dramatic increase in RD values during the post-acute phase, which has been linked to demyelination,<sup>28,32,33</sup> was significantly attenuated in IVIg-treated animals, leading to overall improvements in FA for the VLWM. These findings suggest that IVIg may mediate part of its therapeutic effect by protecting spared axons against secondary immune-mediated demyelination, which is consistent with the observed increases in myelin content in spared white matter of IVIg-treated animals. In further direct agreement, RD values were highly correlated to myelin content. An additional contributing factor may have been enhanced reparative remyelination following IVIg treatment.<sup>34</sup> DTI did not appear to be sensitive enough to detect more subtle degeneration of axons in the post-acute phase through ongoing changes in AD values, at least not under the imaging conditions used. Given that our postmortem histopathological analysis suggests that IVIg therapy might preserve and/or prevent the degeneration of at least some compromised axons, future studies should test other DTI protocols that may be more optimally designed to detect changes in AD.<sup>35</sup> Regardless, our results show that DTI is not only useful for monitoring lesion development, but that it can also provide clues on the putative mechanism of action for

therapeutic interventions through differential changes in diffusion indices (in this case RD). FA and RD values for the VF at the study endpoint also directly correlated with the neurological outcome, with a similar trend observed for the LF. These results thus indicate that FA and RD values can act as useful biomarkers in SCI for VLWM integrity and for monitoring the extent of secondary degenerative changes over time, either in the presence or absence of a therapeutic intervention.

In addition to establishing IVIg's dose–response relationship and exploring the use of DTI to noninvasively study treatment efficacy, we also demonstrated acute reductions in the presence of complement activation products within the injured neural parenchyma following IVIg therapy, specifically C5a and C3b/iC3b. These findings are important from a clinical perspective as excessive and indiscriminate complement activation, triggered by trauma and associated bleeding<sup>36</sup> contributes significantly to secondary inflammatory pathology via “innocent bystander” effects in various forms of acquired CNS injury, including SCI.<sup>36,37</sup> We recently provided direct evidence for this by showing that the complement activation product C5a drives pro-inflammatory cytokine production after SCI, and that inhibition of the main signaling receptor for C5a (C5aR1) during the subacute phase of injury improves outcomes.<sup>14</sup> The observed reductions in complement activation products within the spinal cord with IVIg therapy may appear somewhat counterintuitive at first sight based on the well-established link between Ig and classical pathway initiation. It is important to distinguish, however, between the opposing roles of natural (non-self) versus pathogenic (self-reactive) antibodies in relation to complement activation and SCI or TBI outcomes.<sup>6,13,38</sup> *In vivo* scavenging of C3-derived active fragments by exogenously administered natural immunoglobulins is likely to not only reduce terminal complement pathway activation but also CR2 signaling in B cells, thereby inhibiting production of IgM antibodies that could otherwise react with neoepitopes exposed by CNS injury.<sup>38</sup> In combination, these findings highlight the validity of two immunomodulatory strategies to reduce inflammatory pathology following neurotrauma: (1) boosting natural nonpathogenic antibody titers by therapies like IVIg, or (2) use of more targeted complement inhibitors<sup>14,39</sup>; both suppress harmful effects of adaptive immune activation, pathogenic antibody production and/or complement activation.<sup>23,40</sup>

Other mechanisms for IVIg's effectiveness in acquired CNS injury may involve F<sub>c</sub> receptor-dependent actions,<sup>12</sup> with the net result of these interactions being attenuated endothelial cell dysfunction<sup>41</sup> and increased neuronal survival.<sup>42</sup> Proposed mechanisms via which IVIg may exert its anti-inflammatory effects is by suppressing the expression of activating F<sub>c</sub> receptors on macrophages



while increasing the levels of inhibitory F<sub>c</sub> receptor on these cells. Our observation that IVIg therapy led to a significant reduction in the number of phagocytically active (Iba1<sup>+</sup>CD68<sup>+</sup>) macrophages at and around the site of SCI is particularly interesting in this regard and requires further investigation. Aside from leukocytes, F<sub>c</sub> receptor expression has also been reported on neurons, astrocytes, oligodendrocytes, and microglia.<sup>43</sup> A clear localization/binding of intravenously administered hu-IgG to these neural cell types was observed at 1 day post-SCI when integrity of the blood–spinal cord barrier is dramatically disrupted.<sup>44</sup> The putative significance of these interactions for neuroprotection and/or repair remains unclear,<sup>12</sup> although a previous report has shown that cross-linking of F<sub>c</sub>γ receptor by IgG can lead to the activation and differentiation of oligodendrocyte precursor cells,<sup>45</sup> which may have aided repair *in vivo*.

Intriguingly, several recent studies have demonstrated direct crosstalk between complement and F<sub>c</sub> receptor signaling. Specifically, C5a induces robust upregulation of activating F<sub>c</sub> receptors and downregulation of the inhibitory F<sub>c</sub>γRIIB on effector macrophages,<sup>46</sup> thereby lowering their activation threshold. Treatment with IVIg blocks these effects of C5a on macrophages,<sup>47</sup> possibly through the direct scavenging/neutralization of this complement activation product.<sup>10</sup> The complex interplay between complement and FcR signaling (and the influence of IVIg thereon) requires further investigation as the inhibitory F<sub>c</sub>γRIIB can also block C5a signaling events downstream of C5aR1 through its interaction with Dectin-1.<sup>48</sup> IVIg may thus also act through F<sub>c</sub> receptor-dependent mechanisms that are interlinked with complement activation. Regardless of the precise mechanism(s) of action, the repurposing of IVIg for the scavenging/neutralization of harmful complement activation products such as C5a warrants serious consideration for clinical phase investigations in acute SCI.

As some studies have suggested that the addition of a protein reserve *per se* may be neuroprotective,<sup>22</sup> we lastly assessed the effect of albumin treatment to control for protein loading. Consistent with previous reports that have ascribed some immunosuppressive<sup>49</sup> and/or antioxidant properties<sup>50</sup> to high-dose albumin treatment in CNS injury, modestly improved SCI outcomes were observed but these were inferior compared to IVIg therapy. These differences may be explained by the fact that, although albumin treatment had a modest impact on lesion volume, length, and myelin content, no significant reduction in the CD11b<sup>+</sup> infiltrate at the lesion site, as seen with IVIg, was observed.

Lastly, although we are not aware of published evidence showing an influence of neuroprotective sex hormones like progesterone<sup>51</sup> on complement system activation and/or the benefits of IVIg therapy, it is important to point out that we conducted our study exclusively in

female mice because of the higher incidence of mortality and adverse events in males, for example, from urosepsis.

In conclusion, the present findings highlight the potential of IVIg as a readily available and promising immunomodulatory treatment to improve the prospects of recovery from acute SCI. Considering that IVIg already has a good established safety profile,<sup>5</sup> rapid translation to explore its efficacy in human patients is warranted, particularly in individuals with (anatomically) incomplete SCI. We have also demonstrated that DTI, a noninvasive and clinically relevant imaging technique, is capable of detecting microstructural differences/improvements in the integrity of spinal cord white matter, in particular with regard to RD values. Routine incorporation of DTI techniques, both clinically and in translational SCI research, could therefore prove extremely advantageous, not only for characterizing SCI pathology and/or stratification of suitable patients but also to expedite the selection and validation of the most promising therapeutics in clinical trials.

## Acknowledgments

The authors thank Dr. Adrian Zuercher (CSL Ltd. Bio21 Institute & CSL Behring) and Dr. Martin Pearce (CSL Ltd. Bio21 Institute) for their efforts to provide the IVIg preparations that enabled this work. They also thank Mr. Luke Hammond and Ms. Andrea Maher for technical assistance, University of Queensland Biological Resources staff for maintaining mouse colonies, and Ms. Rowan Tweedale (Queensland Brain Institute) for critical appraisal and editorial assistance. Lastly, the authors gratefully acknowledge the Queensland Government for operational funding support of the 16.4 T NMR spectrometer (QLD NMR Network Initiative).

## Author contributions

F.H.B, N.D.K, J.V., P.F.B., F.K., T.V.A., M.B., and M.J.R designed research, F.H.B, N.D.K, J.V., and M.J.R performed research, F.H.B. and M.J.R analyzed data. F.H.B. and M.J.R wrote the paper. All authors read and approved the final manuscript.

## Conflict of Interest

F.K. is an employee of CSL Behring AG (Bern, Switzerland). M.B. is the President of BioVisions Inc. These authors supplied IVIg and/or contributed to study design. The described experimental studies, including all aspects of data collection and analysis, were conducted independently in the laboratory of M.J.R. at The University of Queensland.

## References

- Donnelly DJ, Popovich PG. Inflammation and its role in neuroprotection, axonal regeneration and functional recovery after spinal cord injury. *Exp Neurol* 2008;209:378–388.
- Ducker TB, Zeidman SM. Spinal cord injury. Role of steroid therapy. *Spine (Phila Pa 1976)* 1994;19:2281–2287.
- Miller SM. Methylprednisolone in acute spinal cord injury : a tarnished standard. *J Neurosurg Anesthesiol* 2008;20:140–142.
- Bayry J, Negi VS, Kaveri SV. Intravenous immunoglobulin therapy in rheumatic diseases. *Nat Rev Rheumatol* 2011;7:349–359.
- Katz U, Achiron A, Sherer Y, et al. Safety of intravenous immunoglobulin (IVIg) therapy. *Autoimmun Rev* 2007;6:257–259.
- Basta M. Ambivalent effect of immunoglobulins on the complement system: activation versus inhibition. *Mol Immunol* 2008;45:4073–4079.
- Basta M, Dalakas MC. High-dose intravenous immunoglobulin exerts its beneficial effect in patients with dermatomyositis by blocking endomysial deposition of activated complement fragments. *J Clin Invest* 1994;94:1729–1735.
- Basta M, Kirshbom P, Frank MM, et al. Mechanism of therapeutic effect of high-dose intravenous immunoglobulin. Attenuation of acute, complement-dependent immune damage in a guinea pig model. *J Clin Invest* 1989;84:1974–1981.
- Basta M, Langlois PF, Marques M, et al. High-dose intravenous immunoglobulin modifies complement-mediated in vivo clearance. *Blood* 1989;74:326–333.
- Basta M, Van Goor F, Luccioli S, et al. F(ab)<sup>2</sup>-mediated neutralization of C3a and C5a anaphylatoxins: a novel effector function of immunoglobulins. *Nat Med* 2003;9:431–438.
- Spycher M, Matozan K, Minnig K, et al. In vitro comparison of the complement-scavenging capacity of different intravenous immunoglobulin preparations. *Vox Sang* 2009;97:348–354.
- Schwab I, Nimmerjahn F. Intravenous immunoglobulin therapy: how does IgG modulate the immune system? *Nat Rev Immunol* 2013;13:176–189.
- Ankeny DP, Guan Z, Popovich PG. B cells produce pathogenic antibodies and impair recovery after spinal cord injury in mice. *J Clin Invest* 2009;119:2990–2999.
- Brennan FH, Gordon R, Lao HW, et al. The complement receptor C5aR controls acute inflammation and astrogliosis following spinal cord injury. *J Neurosci* 2015;35:6517–6531.
- Brennan FH, Lee JD, Ruitenberg MJ, et al. Therapeutic targeting of complement to modify disease course and improve outcomes in neurological conditions. *Semin Immunol* 2016;. doi:10.1016/j.smim.2016.03.015.
- Nguyen DH, Cho N, Satkunendrarajah K, et al. Immunoglobulin G (IgG) attenuates neuroinflammation and improves neurobehavioral recovery after cervical spinal cord injury. *J Neuroinflammation* 2012;9:224.
- Dvorak MF, Noonan VK, Fallah N, et al. Minimizing errors in acute traumatic spinal cord injury trials by acknowledging the heterogeneity of spinal cord anatomy and injury severity: an observational Canadian cohort analysis. *J Neurotrauma* 2014;31:1540–1547.
- Carpenter RS, Kigerl KA, Marbourg JM, et al. Traumatic spinal cord injury in mice with human immune systems. *Exp Neurol* 2015;271:432–444.
- Courtine G, Bunge MB, Fawcett JW, et al. Can experiments in nonhuman primates expedite the translation of treatments for spinal cord injury in humans? *Nat Med* 2007;13:561–566.
- Brennan FH, Cowin GJ, Kurniawan ND, et al. Longitudinal assessment of white matter pathology in the injured mouse spinal cord through ultra-high field (16.4 T) in vivo diffusion tensor imaging. *NeuroImage* 2013;82:574–585.
- Song SK, Yoshino J, Le TQ, et al. Demyelination increases radial diffusivity in corpus callosum of mouse brain. *NeuroImage* 2005;26:132–140.
- Cain LD, Nie L, Hughes MG, et al. Serum albumin improves recovery from spinal cord injury. *J Neurosci Res* 2007;85:1558–1567.
- Arumugam TV, Tang SC, Lathia JD, et al. Intravenous immunoglobulin (IVIg) protects the brain against experimental stroke by preventing complement-mediated neuronal cell death. *Proc Natl Acad Sci U S A* 2007;104:14104–14109.
- Chen B, Yoon JS, Hu B, et al. High-dose intravenous immunoglobulin exerts neuroprotective effect in the rat model of neonatal asphyxia. *Pediatr Res* 2014;75:612–617.
- Jeong S, Lei B, Wang H, et al. Intravenous immunoglobulin G improves neurobehavioral and histological outcomes after traumatic brain injury in mice. *J Neuroimmunol* 2014;276:112–118.
- Radojicic M, Nistor G, Keirstead HS. Ascending central canal dilation and progressive ependymal disruption in a contusion model of rodent chronic spinal cord injury. *BMC Neurol* 2007;7:30.
- Gensel JC, Donnelly DJ, Popovich PG. Spinal cord injury therapies in humans: an overview of current clinical trials and their potential effects on intrinsic CNS macrophages. *Expert Opin Ther Targets* 2011;15:505–518.
- Loy DN, Kim JH, Xie M, et al. Diffusion tensor imaging predicts hyperacute spinal cord injury severity. *J Neurotrauma* 2007;24:979–990.
- Kim JH, Loy DN, Wang Q, et al. Diffusion tensor imaging at 3 hours after traumatic spinal cord injury predicts long-term locomotor recovery. *J Neurotrauma* 2010;27:587–598.

30. Kelley BJ, Harel NY, Kim CY, et al. Diffusion tensor imaging as a predictor of locomotor function after experimental spinal cord injury and recovery. *J Neurotrauma* 2014;31:1362–1373.
31. Sundgren PC, Dong Q, Gomez-Hassan D, et al. Diffusion tensor imaging of the brain: review of clinical applications. *Neuroradiology* 2004;46:339–350.
32. Mulcahey MJ, Samdani A, Gaughan J, et al. Diffusion tensor imaging in pediatric spinal cord injury: preliminary examination of reliability and clinical correlation. *Spine (Phila Pa 1976)* 2012;37:E797–E803.
33. Kim JH, Loy DN, Liang HF, et al. Noninvasive diffusion tensor imaging of evolving white matter pathology in a mouse model of acute spinal cord injury. *Magn Reson Med* 2007;58:253–260.
34. Ephrem A, Misra N, Hassan G, et al. Immunomodulation of autoimmune and inflammatory diseases with intravenous immunoglobulin. *Clin Exp Med* 2005;5:135–140.
35. Hui ES, Cheung MM, Chan KC, et al. B-value dependence of DTI quantitation and sensitivity in detecting neural tissue changes. *NeuroImage* 2010;49:2366–2374.
36. Brennan FH, Ruitenber MJ. Targeting acute inflammation to complement spinal cord repair. *Neural Regen Res* 2015;10:1596–1598.
37. Brennan FH, Anderson AJ, Taylor SM, et al. Complement activation in the injured central nervous system: another dual-edged sword? *J Neuroinflammation* 2012;9:137.
38. Neher MD, Rich MC, Keene CN, et al. Deficiency of complement receptors CR2/CR1 in Cr2(-)/(-) mice reduces the extent of secondary brain damage after closed head injury. *J Neuroinflammation* 2014;11:95.
39. Stahel PF, Barnum SR. The role of the complement system in CNS inflammatory diseases. *Expert Rev Clin Immunol* 2006;2:445–456.
40. Neher MD, Weckbach S, Flierl MA, et al. Molecular mechanisms of inflammation and tissue injury after major trauma—is complement the “bad guy”? *J Biomed Sci* 2011;18:90.
41. Widiapradja A, Santro T, Basta M, et al. Intravenous immunoglobulin (IVIg) provides protection against endothelial cell dysfunction and death in ischemic stroke. *Exp Transl Stroke Med* 2014;6:7.
42. Widiapradja A, Vegh V, Lok KZ, et al. Intravenous immunoglobulin protects neurons against amyloid beta-peptide toxicity and ischemic stroke by attenuating multiple cell death pathways. *J Neurochem* 2012;122:321–332.
43. Okun E, Mattson MP, Arumugam TV. Involvement of Fc receptors in disorders of the central nervous system. *Neuromolecular Med* 2010;12:164–178.
44. Popovich PG, Horner PJ, Mullin BB, et al. A quantitative spatial analysis of the blood-spinal cord barrier. I. Permeability changes after experimental spinal contusion injury. *Exp Neurol* 1996;142:258–275.
45. Nakahara J, Tan-Takeuchi K, Seiwa C, et al. Signaling via immunoglobulin Fc receptors induces oligodendrocyte precursor cell differentiation. *Dev Cell* 2003;4:841–852.
46. Shushakova N, Skokowa J, Schulman J, et al. C5a anaphylatoxin is a major regulator of activating versus inhibitory FcγRs in immune complex-induced lung disease. *J Clin Invest* 2002;110:1823–1830.
47. Konrad S, Baumann U, Schmidt RE, et al. Intravenous immunoglobulin (IVIg)-mediated neutralisation of C5a: a direct mechanism of IVIG in the maintenance of a high FcγRIIB to FcγRIII expression ratio on macrophages. *Br J Haematol* 2006;134:345–347.
48. Karsten CM, Pandey MK, Figge J, et al. Anti-inflammatory activity of IgG1 mediated by Fc galactosylation and association of FcγRIIB and dectin-1. *Nat Med* 2012;18:1401–1406.
49. Bar-Or D, Thomas GW, Bar-Or R, et al. Commercial human albumin preparations for clinical use are immunosuppressive in vitro. *Crit Care Med* 2006;34:1707–1712.
50. Belayev L, Saul I, Huh PW, et al. Neuroprotective effect of high-dose albumin therapy against global ischemic brain injury in rats. *Brain Res* 1999;845:107–111.
51. Thomas AJ, Nockels RP, Pan HQ, et al. Progesterone is neuroprotective after acute experimental spinal cord trauma in rats. *Spine (Phila Pa 1976)* 1999;24:2134–2138.

## Supporting Information

Additional Supporting Information may be found online in the supporting information tab for this article:

**Data S1.** Supplementary Methods and References

**Figure S1.** Analysis of central canal dilation

**Table S1.** Injury parameters for mouse cohorts in functional studies